CHEMISTRY
A EUROPEAN JOURNAL

DOI: 10.1002/chem.200800032

Confinement in Nanopores at the Oxide/Water Interface: Modification of Alumina Adsorption Properties

Manuel Baca,[a, b] Xavier Carrier,[a, b] and Juliette Blanchard*[a, b]

Abstract: There is limited knowledge on the influence of the pore size on surface phenomena (adsorption, dissolution, precipitation, etc.) at the oxide/water interface and a better understanding of the space confinement in nanoscale pores should have practical implications in different areas, such as transport of contaminants in the environment or heterogeneous catalyst preparation, to name a few. To investigate the modifications of the oxide adsorption properties at the oxide/water interface in a confined environment, the surface acidobasic and ion adsorption properties of six different aluminas (5 porous commercial aluminas with pore diameters ranging from 25 to 200 Å and 1 non-porous alumina) were determined by means of acid–base titration and Ni(II) adsorption. It is shown that the confinement has a moderate impact on the alumina adsorption capacity because all materials have similar surface charging behaviours and ion saturation coverages. However, a confined geometry has a much larger impact on the ion adsorption constants, which decrease drastically when the average pore diameter decreases below 200 Å. These results are discussed in terms of nanoscale pore space confinement.

Keywords: adsorption · alumina · pore-size effect · supported catalysts · surface chemistry

Introduction

The confinement of water in nanoporous materials is the subject of intense research due to its potential impact in various fields, including soil science, heterogeneous catalysis, materials science and biological processes.[1] The terminology "confinement" is used when the porosity induces a modification of the physicochemical properties (phase behaviour, molecular mobility, etc.) of molecules or solutes present (confined) in the pores. For example, it is well known that the water solidification transition is always lower in nanopores than in bulk solution. Experimental evidence has been given by using mesoporous silica-based materials,[2,3] such as MCM-41 with pore diameters ranging from 20 to 40 Å and it was shown that water solidifies 50 K below its bulk value. The dielectric constant (ε) of water (and thus its dissociation properties) can also be drastically modified in a confined space as demonstrated by using molecular dynamics simulations, which showed that ε decreases by 50% when water is confined in a pore of 12 Å.[4] Extending these results to the oxide/water interface, one may therefore expect that adsorption of molecules/ions on oxide surfaces, which is largely dictated by the properties of interfacial water, will be dependent on the porosity of the oxide adsorbent. Surprisingly, very little data is available to confirm this hypothesis, despite practical implications for the transport of contaminants in the environment or heterogeneous catalyst preparation, for example.[5,6] Only recently, Wang et al. published two papers that provided new insights into the modifications of the ion adsorption properties of alumina supports caused by space confinement.[7,8] They showed first that the surface charge density of a commercial mesoporous alumina ($Ø$ = 6.5 nm) was 45 times higher than a commercial alumina (crushed extrudates) and explained this effect by a significant reduction in the separation of surface OH acidic constants ($\Delta pK = pK_{a_2} - pK_{a_1}$) in a mesopore. As a matter of fact, a narrowing of ΔpK results in a higher concentration of charged surface groups for a given pH. The authors proposed that variations in ΔpK were due to the overlap of the electric double layer (EDL) in mesopores because a pore

[a] Dr. M. Baca, Dr. X. Carrier, Dr. J. Blanchard
UPMC Univ Paris 06, UMR 7609
Laboratoire de Réactivité de Surface
75005, Paris (France)
Fax: (+33) 144-276-033
E-mail: juliette.blanchard@upmc.fr

[b] Dr. M. Baca, Dr. X. Carrier, Dr. J. Blanchard
CNRS, UMR 7609
Laboratoire de Réactivité de Surface
75005, Paris (France)

Supporting information for this article is available on the WWW under http://www.chemeurj.org/ or from the author.

radius in the nm range is comparable to the EDL thickness. However, it was noted by the authors that the effect of EDL overlap cannot be fully integrated in existing surface complexation models.[7] In accordance with the modification of the surface charge, it was also shown by the same authors that the zinc(II) sorption coefficient was approximately 10-fold higher on mesoporous alumina than on conventional alumina extrudates.[7] This drastic increase is obviously the result of the enhanced surface charge on the mesoporous support. But it was also proposed by the authors that the increase may result from a reduction of the activity of water inside a nanopore when considering that reduced activity will decrease the ion hydration and in turn increase the tendency for inner-sphere complexation.[8]

Unfortunately, the work of Wang et al.[7,8] was limited to one type of commercial mesoporous alumina with only one pore size and limited knowledge of the structure of the material. Furthermore, another recent work by Goyne et al.[9] challenged the main conclusions of Wang et al.[7,8] since they showed that silica and alumina materials with variable porosity exhibit identical surface charge behaviour when normalised to the surface area. Hence, the present work aimed at broadening the study of nanopore confinement to a variety of porous commercial transition aluminas with average pore sizes ranging from 20 to 200 Å and a non-porous alumina (pore diameter > 500 Å). To study the impact of pore space confinement, the surface acidobasic properties and the adsorption capacity for a Ni cationic complex were studied for the various alumina materials.

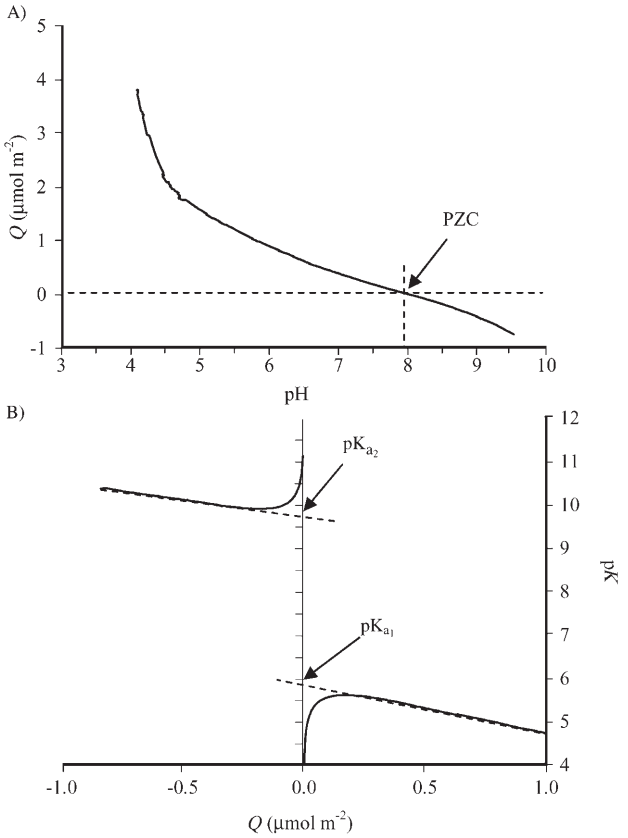

Figure 1. A) Surface charge density calculated from the titration curve. PZC = point of zero charge. B) Acidity constants calculated from the Q versus pH curve for Puralox γ-alumina. Extrapolation of the pK curve to $Q=0$ gives intrinsic acidity constants: pK_{a_1} and pK_{a_2} reported in Table 1.

Results

Surface charge and pK_a values: The evolution of the surface charge (Q) as a function of pH deduced from the potentiometric titration of the Puralox γ-alumina is presented in Figure 1A along with the point of zero charge (PZC) obtained at $Q=0$. A linear extrapolation of the pK versus Q curve to $Q=0$ gives values of the intrinsic acidity constants (pK_{a_1} and pK_{a_2}, Figure 1B). The PZC and intrinsic acidity constants obtained by the same procedure for 6 different transition alumina with pore sizes from 20 to more than 500 Å are given in Table 1. First of all note that the PZC does not change by more than 0.7 pH units for all of the alumina samples studied with only a slight increase with the average pore diameter. This result is in good agreement with those already published and confirms that the PZC is not affected by the pore size to a large extent.[7,9] Examination of Table 1 also reveals that ΔpK (i.e., pK_{a_2}−pK_{a_1}) also marginally increases (less than 0.9 pK units) with the average pore size. These results are in disagreement with the work of Wang et al. in which a clear enhancement of the surface charge was observed on a mesoporous alumina relative to commercial alumina particles.[7,8] To highlight the difference with the work of Wang et al.,[7,8] the surface charge as a function of pH−PZC is plotted in Figure 2 for three different alumina samples. It is shown that, for a given pH, the surface charge per m^2 does not change significantly from one alumina to another, which therefore confirms that the surface charge is almost independent of the average pore size for a given material.

Adsorption capacity: The adsorption isotherm at room temperature of $[Ni(en)_3]^{2+}$ on Puralox γ-alumina is given in Fig-

Table 1. Textural properties (specific surface area (S_{BET}) and average pore diameter ($Ø_{pores}$)) and surface charge behaviour (PZC and intrinsic acidity constants (pK_{a_i})) of the aluminas used in this work.

Sample	Supplier	S_{BET} [m^{2}g^{-1}]	$Ø_{pores}$ ($W_{1/2}$)[a] [Å]	PZC	pK_{a_2}	pK_{a_1}	ΔpK_a
η ETA	Sasol	270	26–18	7.4	9.65	5.25	4.40
η Versal B	UOP	220	27–18	7.4	9.50	5.30	4.20
γ Puralox	Sasol	192	55–38	7.9	9.60	5.85	3.75
γ Ec1520	Axens-IFP	223	67–39	7.6	9.45	5.70	3.75
δ Baikalox	Baikowski	106	200–156	8.1	9.85	6.25	3.60
δ AluC	Degussa	105	> 500[b]	8.0	9.75	6.20	3.55

[a] $W_{1/2}$ = full width at half maximum of the pore size distribution (BJH calculation on the adsorption curve). [b] No maximum in the adsorption curve was found for this sample.

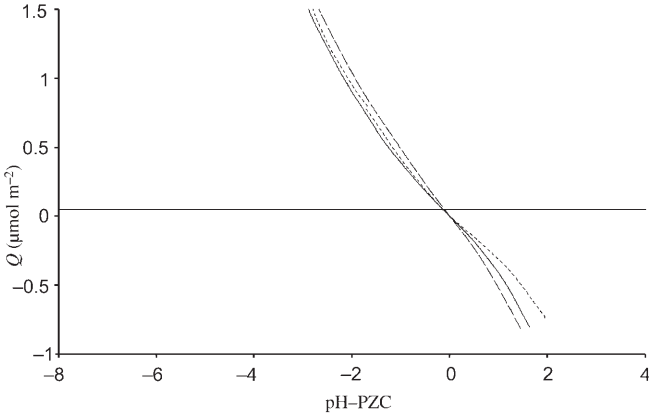

Figure 2. Surface charge density (Q) as a function of pH−PZC for Puralox (——), AluC (-----) and VersalB (•••••) aluminas.

ure 3A. The surface density of adsorbed complexes (Ni_{ads}; in $\mu mol\,m^{-2}$) is plotted as a function of Ni concentration in solution at equilibrium (Ni_{eq}; in $mmol\,L^{-1}$). The shape of the adsorption isotherm suggests Langmuir-type behaviour, with adsorption on a limited number of equivalent adsorption sites.[10] The adsorption isotherms obtained for all the aluminas studied are similar. To confirm the site-adsorption hypothesis, Langmuir transforms of the isotherms were plotted (Figure 3B) and the adsorption constant (K_{ads} in M^{-1}) and Ni saturation coverage ($[S]_{tot}$ in atoms per nm^2) were obtained from b/a and $1/b$, respectively, in which a is the slope and b is the y intercept of the linear regression (Table 2).[10]

Table 2. Adsorption constants (K_{ads}) and Ni saturation coverage ($[S]_{tot}$) determined by linear transform of the adsorption isotherms of $[Ni(en)_3]^{2+}$ on aluminas with various average pore size.[a]

Sample	$Ø_{pores}$ [Å]	K_{ads} [M^{-1}]	$[S]_{tot}$ [atoms per nm^2]
η ETA	26±9	64±9	0.50±0.05
η Versal B	27±9	124±16	0.51±0.04
γ Puralox	55±19	191±23	0.49±0.03
γ Ec1520	67±19	244±33	0.46±0.04
δ Baikalox	186±78	484±74	0.48±0.03
δ-AluC	>500	389±53	0.50±0.03

[a] The uncertainty on the pore diameter was taken as $\pm W_{1/2}$ in which $W_{1/2}$ is the full width at half maximum of the pore size distribution (adsorption curve). The uncertainty on $[S]_{tot}$ was taken as $\pm\sigma_b/b^2$ and the uncertainty on K_{ads} was taken as $\Delta K_{ads} = \pm\frac{a\sigma_b + b\sigma_a}{a^2}$, in which a and b are the slope and the y intercept of the linear regression, respectively, and σ_a and σ_b are their standard deviations.

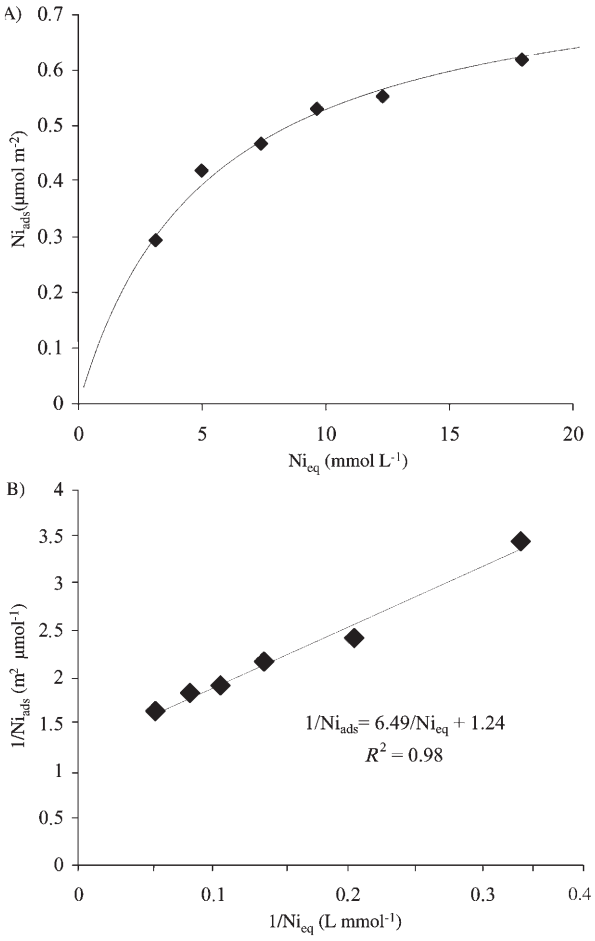

Figure 3. A) Adsorption isotherm of $[Ni(en)_3]^{2+}$ on the Puralox γ-alumina and B) the corresponding linear transform.

The evolution of the adsorption constant and the Ni saturation coverage as a function of the average pore size is plotted in Figure 4. The Ni saturation coverage is approximately identical for each alumina sample at about 0.5 atoms per nm^2. This similarity confirms that the surface chemistry (structure and composition) of the various aluminas used in this work is comparable (in agreement with the fact that their crystallographic structures are closely related). The main distinction between the different oxide supports lies, therefore, only in their pore diameters. Moreover, if one assumes that the adsorption of $[Ni(en)_3]^{2+}$ is purely electrostatic (surface–complex ions pairs) due to the thermodynam-

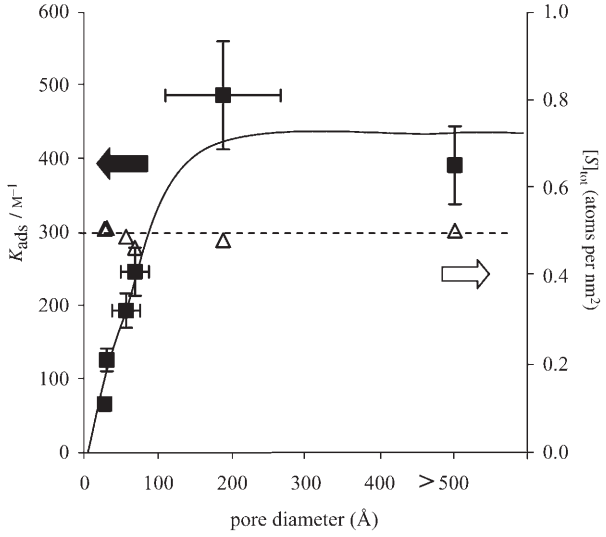

Figure 4. Evolution of the adsorption constant (K_{ads}; ■) and the saturation coverage ($[S]_{tot}$; △) versus the average pore diameter.

ic stability and kinetic inertness of chelate complexes,[11,12] the identical saturation coverages obtained clearly confirms the results obtained by acid–base titrations, that is, the surface charge, and thus, the ion adsorption capacity does not depend on the average pore size.

Conversely, with regards to the evolution of the adsorption constant (K_{ads}), Figure 4 clearly demonstrates that the pore size has a drastic effect. One can observe a regular increase in K_{ads} with the pore size for pore diameters up to 100 Å. From a quantitative point of view, the adsorption constant estimated for the Baikalox δ-alumina (average pore size of 186 Å) and for the AluC δ-alumina (pore size >500 Å) is six to seven times higher than that calculated for the η-alumina from Sasol (average pore size of 26 Å). This result implies that the ion adsorption constant is greatly reduced when the pore size decreases.

Discussion

Surface charge and pK_a values: The similarity in PZC and surface charge observed for the different alumina used in this work is in agreement with the work of Lyklema and co-workers.[13] It was shown by these authors that a "universal" curve for surface charge can be obtained for different oxides (i.e., hematite and rutile in their case) when the surface charge is plotted as a function of pH−PZC, that is, when the x coordinate is corrected for differences in the PZC, which depends only on intrinsic acidity constants. As a matter of fact, the determination of a surface OH group acidity constant (pK_a), and thus of a PZC value, is based solely on OH coordination in most existing surface ionisation models, such as the MUSIC model from Hiemstra and co-workers.[14] In this model, the pK_a value depends on the degree of undersaturation of the oxygen charge, which is defined by the number of cations coordinating the oxygen atom, the cation–oxygen bond length and the existence of hydrogen bonds. Hence, this model is surface dependent (composition and structure), but it is unaffected by the pore size. Therefore, according to the MUSIC model, the pK_a (and thus the PZC) of different alumina with the same surface structure should be similar regardless of the pore size, which is in agreement with our results (Table 1) and those of Goyne et al.[9] The slight differences observed among the various transition aluminas (δ, γ, η) are probably related to small variations in the fraction of exposed faces. As a matter of fact, all of the transition aluminas used in this work have a similar crystallographic structure based on face-centred cubic compact oxygen packing, but η-Al_2O_3 is obtained by dehydration of bayerite, whereas γ-Al_2O_3 and δ-Al_2O_3 are obtained from boehmite at different temperatures.[15] Hence, the last two alumina should have surface properties closer to each other than the first one. Accordingly, the PZC of γ-Al_2O_3 and δ-Al_2O_3 are very close (7.6 to 7.9 for the γ-aluminas, 8.0 to 8.1 for the δ-aluminas) and slightly higher than that of η-Al_2O_3 (7.4). As a matter of fact, the similar surface properties of the different alumina are also revealed by a comparable number of total adsorption sites as shown above (Table 2).

Nevertheless, one can still anticipate that materials with identical surface properties (PZC and intrinsic pK_a), but with different porosities may well develop different surface charges. Lyklema and co-workers, claimed that the surface charge has generic behaviour (as opposed to PZC, which is oxide specific) that is only governed by the solution side of the double layer.[13] This assertion can be translated into thermodynamic terms by breaking down the free energy [Eq. (1)], or the acidity constants [Eq. (2)], of protonation/deprotonation of surface OH groups into oxide-specific (intrinsic) and coulombic (generic) terms:[10]

$$\Delta G^0_{app} = \Delta G^0_{intr} + \Delta G^0_{coul} \quad (1)$$

$$K_{a_{app}} = K_{a_{intr}} K_{a_{coul}} \quad (2)$$

ΔG^0_{app} (or $K_{a_{app}}$) is the apparent (microscopic) free energy of protonation/deprotonation that is actually measured at each point on the titration curve (Figure 1B). ΔG^0_{intr} is the intrinsic free energy of protonation/deprotonation, which is an oxide-specific property (i.e., intrinsic K_a) measured at $Q=0$ that does not depend on the surface charge, whereas ΔG^0_{coul} is a generic electrostatic term for all oxides and depends on the solution properties (the solution side of the EDL). ΔG^0_{coul} reflects the electrostatic work in transporting ions through the interfacial potential gradient (Ψ). In other words, it means that it is more and more difficult to protonate a positively charged surface as the charge increases. The coulombic term (related to the surface potential through $\Delta G^0_{coul} = ZF\Psi$, in which F is the Faraday constant and Z is the change in the charge of the surface species) should be roughly identical for different oxides at a given pH−PZC value and ionic strength.[10] These considerations easily explain why Lyklema and co-workers obtained a "universal" curve for surface charge versus pH−PZC for different oxides.[13]

However, the preceding considerations neglect the possibility that porosity could also play a role. As a matter of fact, as mentioned earlier by Wang et al.,[7] for ionic strengths between 0.01 and 0.1 M, the EDL thickness is in the mesoporosity range (3 and 1 nm, respectively) and a significant overlap of the EDL can occur in nanopores. Such an overlap, will in turn lead to an enhanced interfacial potential gradient in the porosity and consequently an increased contribution of ΔG^0_{coul} when compared with a planar surface. Qualitatively speaking, a proton will have to overcome a higher surface potential to be adsorbed on a partially protonated surface. Hence, on a qualitative basis, one can suppose that the apparent acidic constants for deprotonation (K_{a_1}) of a confined pore will be higher (i.e., lower pK_{a1}) than that of a planar surface and result in a lower surface charge for mesoporous materials. Note that Zhmud et al.[16,17] also postulated that the surface charge of mesoporous materials should decrease with the pore size based on a different approach.

This hypothesis differs from the work performed by Wang et al.[7] in which it is shown that the surface charge is enhanced for a mesoporous material with respect to commercial alumina particles. However, this conclusion is drawn from the comparison of only two aluminas of unknown pore size distribution and, for one of them, of poor crystallinity.

As mentioned above, the absence of a clear confinement effect on the surface charge for the various aluminas used in this work is not definite proof that the surface charge is unaffected by the porosity. The results obtained herein are restricted to the conditions and materials used. For example, we postulated above that one of the possible effects of a confined pore is to lead to the overlap of the EDL. The thickness of the EDL is extremely dependent on the ionic strength: the higher the ionic strength, the shorter the EDL. Hence, we can suggest that a clear effect of confinement would only be observed for very low ionic strength (i.e., large EDL thickness), whereas for higher ionic strength (i.e., 0.1 M) the EDL thickness is too low (ca. 1 nm[10]) to lead to a significant overlap in the mesopores of the aluminas we have investigated. Hence, we believe that, to conclude unambiguously, the present work should be extended to titrations with variable ionic strength and/or to mesoporous alumina with smaller pore sizes.

Ion adsorption constants K_{ads}: The increase in the ion adsorption constant by a factor of six to seven between the smaller (26 Å) and the larger (200 Å and >500 Å) pores cannot be assigned to minor modifications of the crystallographic structure of the different transition alumina because within a given crystallographic structure (η, γ) a clear effect of the pore diameter is always observed. Another possible explanation for the low adsorption constant for small pore diameters may lie in the slow diffusion of Ni complexes in the smaller pores. However, this hypothesis is very unlikely considering the equilibration time (15 h) used in this series of experiments. As a matter of fact, it was shown by van de Water et al.[18] by means of UV/Vis microspectroscopy that 5 min were enough for detecting Ni ions at the core of 3 mm γ-Al_2O_3 pellets initially impregnated with an acidified solution of Ni–ethylenediamine and Wang et al.[7] reported that the ion uptake in a mesoporous alumina, although longer than in conventional alumina, occurred within a few minutes. Moreover, an equilibration time higher than 15 h would result in a profound modification of the surface properties of the alumina used in this work because it was shown previously that $Al(OH)_3$ precipitation could be observed in as little as 24 h.[19] Hence, the contact time used in this work results from the trade-off between the necessary diffusion of Ni complexes and the unwanted alumina alteration in aqueous solution.

The reduction in the adsorption constant with the pore size could only be explained by a modification of the solvent properties in the porosity, since the surface charge is comparable for different pore sizes (see above). As a matter of fact, it was reported by Zhmud et al. that a charged surface may influence the association constant (K_{as}) of an ion pair, that is, the adsorption of a cation on a negatively charged surface group, by modifying the permittivity of the solution close to the surface.[16] Indeed the permittivity (i.e., the dielectric constant) of a solvent is lower near a charged surface than in the bulk. In turn, the dehydration energy is lower and the formation of an ion pair, which requires dehydration of both ions, involves less energy and the association constant should be higher. Without the need to consider a charged interface, this effect can even be enhanced when the solvent is confined in a nanopore. Senapati and Chandra have shown, with the help of molecular dynamics simulations, that the confinement of water in an uncharged nanopore 12 Å in diameter resulted in a 50% decrease in the dielectric constant with respect to bulk water.[4] Hence, one may expect that the formation of an ion pair is even more favourable in small pores. A similar proposition for inner-sphere adsorption was made by Wang et al. considering the water activity in a confined pore.[8] The authors noted that the activity of water can be much lower in a nanopore (following Kelvin's equation, the activity is proportional to r^{-1}), which results in a lower hydration of aqueous species, and hence, a stronger tendency for inner-sphere surface complexation.

However, our experimental results are opposed to the preceding hypotheses because the adsorption constant measured for the adsorption of $[Ni(en)_3]^{2+}$ on various alumina samples is disfavoured for decreasing pore sizes. This discrepancy may indicate that the adsorption of $[Ni(en)_3]^{2+}$ is more complicated than a simple ion pair formation. In fact, Boujday et al. have shown that a complete description of adsorption sites for Ni–ethylenediamine complexes on silica requires that the cooperative formation of hydrogen bonds between the Ni^{II} complex and the surface (interactional complementarity) through the interaction of NH groups from ethylenediamine (hydrogen donors) and surface oxygen atoms (hydrogen acceptors) is taken into account.[20] Moreover, it is recognised that the solvent may perturb the intermolecular hydrogen-bonding interactions by competing for hydrogen bonds, depending on the solvent properties,[21] and Monte Carlo simulations are in agreement with a perturbation of the hydrogen-bond network in a confined environment.[22] Hence, one can speculate that the reduced adsorption constants observed in this work for confined pores may result from a reduced tendency for hydrogen bonding caused by a modification of the solvent properties in small pores. However, these notions remain hypotheses at this time and much theoretical and experimental work needs to be done to be able to fully rationalise the influence of confinement at the oxide/water interface.

Conclusion

For the first time, several aluminas with various pore diameters were used to study the modification of the oxide adsorption properties at the oxide/water interface in a confined environment. The pK_a values and the surface charge

densities are not significantly modified by the pore diameter, in agreement with the work of Goyne et al.[9] and the MUSIC model,[14] which considers that the pK_a values (and thus the PZC) depend only on the structure and composition of the oxides. This result is confirmed by $[Ni(en)_3]^{2+}$ adsorption isotherms, which reveal a constant coverage at saturation regardless of the pore size of the alumina. On the other hand, the adsorption constant was increased by a factor of six to seven when the average pore diameter increases from 26 to 200 Å or more. A reverse effect would be expected by considering a reduction in the dielectric constant of water inside the mesopores. One possible explanation is a reduced tendency for hydrogen bonding in mesopores because it is known that the adsorption of $[Ni(en)_3]^{2+}$ is more complicated than simple ion pair formation.[20]

The decrease in the adsorption constant with decreasing pore size could have major consequences for controlling the transport of environmental contaminants and for the preparation of heterogeneous catalysts, and therefore, deserve further investigations. Because the alumina samples used for this study have three different crystallographic structures (η, γ, δ) and relatively broad pore size distributions, it would be interesting to confirm these results and to use model alumina with controlled pore sizes, such as those recently developed by grafting aluminium alkoxides on ordered silica mesoporous supports.[23–25]

Moreover, the work reported herein deals with the adsorption of a cationic metal complex. It would also be of utmost importance to broaden this work to the adsorption of oxoanions (such as molybdates, that is, MoO_4^{2-}) because these species are precursors for alumina-based heterogeneous catalysts in the petroleum industry.

Experimental Section

The transition alumina (η, δ, γ) used in this work were obtained from several suppliers with the aim of obtaining a large range of pore sizes while retaining the same chemical composition. All of these samples were calcined at 500 °C for 3 h before use except for the Versal B alumina, which was calcined at 450 °C for 6 h. The source and textural properties of the alumina are summarised in Table 1. The structure of the different materials was confirmed by XRD.[15] BET surface areas and pore diameters were obtained by N_2 adsorption–desorption isotherms with an ASAP 2010 analyzer (Micromeritics). Prior to analysis, the samples were degassed ($p < 1$ Pa) at 250 °C for 5 h. The contribution of micro- and meso-porosity to the overall surface area was estimated from a *t*-plot (Harkin–Jura) analysis of the adsorption curve ($0.3\,nm < t < 0.5\,nm$, in which *t* is the statistical thickness). For the calculation of the pore size distribution and the average pore diameter, the BJH calculation was performed on the adsorption branch due to ink-bottle-shaped pores. For the δ-AluC sample no maximum in the adsorption curve was observed, which indicated that this sample is essentially non-porous.

Potentiometric titrations were conducted by using a TIM 856 titration workstation (Radiometer Analytical) to determine the surface charge, PZC and the pK_{a_i} values ($i = 1$ or 2) of the different alumina. Suspensions were prepared by placing the alumina (250 mg) in contact with a 0.1 M solution of $NaNO_3$ (60 mL). A 0.1 M solution of NaOH (1 mL) was then added and the suspension was stirred under N_2 atmosphere for 15 min. The titration was finally performed with a 0.05 M solution of HNO_3 until a pH of 3 was reached. The values for Q [mol m^{-2}], PZC and pK_{a_i} were calculated from the titration curve with a one-site-two-pK model,[10] (see the Supporting Information).

The ion adsorption properties were studied by means of $[Ni(en)_3]^{2+}$ adsorption. This complex was used because it has several advantages:[26] Firstly, it can be easily prepared stoichiometrically in aqueous solution by adding three equivalent of ethylenediamine to the solution of $NiNO_3$ due to its high formation constant. Secondly, this complex is kinetically inert due to chelate effects, which favour an electrostatic-type adsorption (no modification of the coordination sphere)[11,12] at the expense of surface grafting observed for mono- and bis-ethylenediamine complexes[27] or complex surface reactions (polymerisation, dissolution-precipitation, etc.). Finally, this complex has three well-defined and characteristic bands in the UV/Vis region (343, 540 and 881 nm), which permit rapid and accurate quantitative measurements to be carried out in the liquid state on the supernatant obtained after adsorption. The support (250 mg) was placed in contact with a solution (10 mL) containing increasing concentrations of $[Ni(en)_3]^{2+}$ ($0.005\,M < [Ni] < 0.02\,M$) for 15 h at the natural pH of the solutions (ca. pH 8). The supernatant was then separated by filtration and the Ni concentration in the filtrate was measured by UV/Vis spectroscopy on a Jasco V-550 UV/Vis spectrophotometer using the absorption band at 345 nm.

Acknowledgements

This work was supported by the ANR program JCJC (ANR-05-JCJC-0216-01). The authors acknowledge E. Ambroise for preliminary experiments and J. F. Lambert for stimulating discussions.

[1] *J. Phys.: Condens. Matter, 16*, **2004**, 55297–55449..
[2] K. Morishige, K. Kawano, *J. Chem. Phys.* **1999**, *110*, 4867–4872.
[3] N. Floquet, J. P. Coulomb, N. Dufau, G. Andre, R. Kahn, *Phys. B (Amsterdam, Neth.)* **2004**, *350*, 265–269.
[4] S. Senapati, A. Chandra, *J. Phys. Chem. B* **2001**, *105*, 5106–5109.
[5] G. E. Brown, V. E. Henrich, W. H. Casey, D. L. Clark, C. Eggleston, A. Felmy, D. W. Goodman, M. Gratzel, G. Maciel, M. I. McCarthy, K. H. Nealson, D. A. Sverjensky, M. F. Toney, J. M. Zachara, *Chem. Rev.* **1999**, *99*, 77–174.
[6] K. Bourikas, C. Kordulis, A. Lycourghiotis, *Catal. Rev. Sci. Eng.* **2006**, *48*, 363–444.
[7] Y. Wang, C. Bryan, H. Xu, P. Pohl, Y. Yang, C. J. Brinker, *J. Colloid Interface Sci.* **2002**, *254*, 23–30.
[8] Y. F. Wang, C. Bryan, H. F. Xu, H. Z. Gao, *Geology* **2003**, *31*, 387–390.
[9] K. W. Goyne, A. R. Zimmerman, B. L. Newalkar, S. Komarneni, S. L. Brantley, J. Chorover, *J. Porous. Mater.* **2002**, *9*, 243–256.
[10] W. Stumm, *Chemistry of The Solid-Water Interface: Processes at the Mineral-Water and Particle-Water Interface in Natural Systems*, Wiley, New York, **1992**.
[11] X. Carrier, E. Marceau, M. Che, *Pure Appl. Chem.* **2006**, *78*, 1039–1055.
[12] K. Q. Sun, E. Marceau, M. Che, *Phys. Chem. Chem. Phys.* **2006**, *8*, 1731–1738.
[13] L. G. J. Fokkink, A. Dekeizer, J. Lyklema, *J. Colloid Interface Sci.* **1989**, *127*, 116–131.
[14] T. Hiemstra, H. Yong, W. H. Van Riemsdijk, *Langmuir* **1999**, *15*, 5942–5955.
[15] P. Euzen, P. Raybaud, X. Krokidis, H. Toulhoat, J. L. L. Loarer, J. P. Jolivet, C. Froidefond in *Handbook of Porous Solids* (Eds.: F. Schüth, K. S. W. Sing, J. Weitkamp), Wiley-VCH, Weinheim, **2002**, pp. 1591–1677.
[16] B. V. Zhmud, J. Sonnefeld, W. A. House, *J. Chem. Soc. Faraday Trans.* **1997**, *93*, 3129–3136.
[17] B. V. Zhmud, *J. Colloid Interface Sci.* **1996**, *183*, 111–117.
[18] L. G. A. van de Water, J. A. Bergwerff, T. A. Nijhuis, K. P. de Jong, B. M. Weckhuysen, *J. Am. Chem. Soc.* **2005**, *127*, 5024–5025.

[19] X. Carrier, E. Marceau, J. F. Lambert, M. Che, *J. Colloid Interface Sci.* **2007**, *308*, 429–437.
[20] S. Boujday, J.-F. Lambert, M. Che, *ChemPhysChem* **2004**, *5*, 1003–1013.
[21] J. L. Cook, C. A. Hunter, C. M. R. Low, A. Perez-Velasco, J. G. Vinter, *Angew. Chem.* **2007**, *119*, 3780–3783; *Angew. Chem. Int. Ed.* **2007**, *46*, 3706–3709.
[22] T. Urbic, V. Vlachy, K. A. Dill, *J. Phys. Chem. B* **2006**, *110*, 4963–4970.
[23] P. M. Rao, A. Wolfson, S. Kababya, S. Vega, M. V. Landau, *J. Catal.* **2005**, *232*, 210–225.
[24] M. V. Landau, E. Dafa, M. L. Kaliya, T. Sen, M. Herskowitz, *Microporous Mesoporous Mater.* **2001**, *49*, 65–81.
[25] M. Baca, E. de la Rochefoucauld, E. Ambroise, J.-M. Krafft, R. Hajjar, P. P. Man, X. Carrier, J. Blanchard, *Microporous and Mesoporous Mater.* **2008**, *110*, 232–241.
[26] J. F. Lambert, M. Hoogland, M. Che, *J. Phys. Chem. B* **1997**, *101*, 10347–10355.
[27] F. Négrier, E. Marceau, M. Che, J.-M. Giraudon, L. Gengembre, A. Löfberg, *J. Phys. Chem. B* **2005**, *109*, 2836–2845.

Received: January 8, 2008
Published online: May 21, 2008

